

Water column interleaving: A new physical mechanism determining protist communities and bacterial states

Connie Lovejoy¹

GIROQ, Department of Biology, Université Laval, Québec, Québec G1K 7P4, Canada

Eddy C. Carmack

Fisheries and Oceans, Pacific Region, Institute of Ocean Sciences, Sidney, British Columbia V8L 4B2, Canada

Louis Legendre²

GIROQ, Department of Biology, Université Laval, Québec, Québec G1K 7P4, Canada

Neil M. Price

Department of Biology, McGill University, 1205 Avenue Docteur Penfield, Montreal, Quebec H3A 1B1, Canada

Abstract

During a spring–summer bloom in a large Arctic polynya, vertically distinct protist communities (phytoplankton and protozoa) occurred within layers caused by interleaving and entrainment of different water masses. We developed a ternary community distance index to quantify the variability in protist community structure in these heterogeneous surface layers. This index was highly correlated ($r = 0.984$, $n = 6$) with the extent of physical interleaving (quantified as the root mean square deviations in temperature between measured and smoothed profiles) indicating a high degree of physical–biotic coupling within water columns of the polynya. Water mass layering created favorable conditions for ciliate blooms. These blooms were associated with distinct temperature–salinity layers. These layers might act as processing traps for particulate organic matter, with highest concentrations of viruses and bacteria (specifically cells with open or leaky membranes, suggesting microbial grazing pressure) occurring in highly interleaved water columns. In contrast, viral and bacterial concentrations were lowest at a noninterleaved station where protist biomass was dominated by flagellates and small dinoflagellates that were evenly distributed down the water column. Water mass interleaving is likely to contribute to microbial biodiversity, community structure and vertical segmentation of biogeochemical processes in the upper ocean.

Water masses can be defined by their temperature (T) and salinity (S) characteristics, which are determined by atmosphere–ocean interactions and freshwater input from rivers or ice melt. Once formed, the waters can be transported away from their site of origin and can be tracked by their distinct

TS signatures. In areas of complex hydrodynamics, waters of similar density but different TS characteristics meet and interleave to form intrusions and isolated lenses. Although these intrusions and lenses might not be evident from sigma-T density profiles, vertically and horizontally varied mixed layers are not unusual (Lal and Lee 1988). In many oceans, “cold fresh” and “warm salty” waters readily interleave (May and Kelley 2001). Although much documented evidence of this phenomenon is from deeper waters, inspection of TS profiles shows that the phenomenon also occurs in the upper 100 m and is therefore relevant to biological processes in the upper ocean (Bâcle et al. 2002).

Horizontal patchiness of protist communities (phytoplankton and protozoa) is recognized as an important factor contributing to uncertainties in estimates of global carbon fixation, and variations in vertical structure have been suggested as being equally important (Sathyendranath et al. 1995). Variations in the vertical distributions of chlorophyll *a* (Chl *a*) with depth is well documented (Richardson et al. 1985; Barth et al. 2001), and there is increasing evidence for distinct vertical and horizontal variability in the distribution of major algal groups (Wright and van den Enden 2000). However, analysis of protist community structure is rare, in part because species data can only be obtained from direct microscopic examination, which is labor intensive and requires taxonomic expertise.

Fronts and intrusions can result in internal resuspension

¹ To whom correspondence should be addressed. Present address: Institut de Ciències del Mar, CMIMA, Passeig Marítim de la Barceloneta 37-49, 08003, Barcelona, Catalonia, Spain (connie.lovejoy@giroq.ulaval.ca or clovejoy@icm.csic.es).

² Present address: Laboratoire d’Océanographie de Villefranche, BP 28, 06234 Villefranche-sur-Mer Cedex, France.

Acknowledgments

This paper is a contribution to the International North Water Polynya Study led by Louis Fortier and funded by the Natural Sciences and Engineering Research Council of Canada (NSERC) and the Department of Fisheries and Oceans Canada. NSERC and Fonds FCAR Québec also provided support for GIROQ (Groupe interuniversitaire de recherches océanographiques du Québec) and to L.L. C.L. was supported by NSERC postgraduate fellowships throughout the study. Thanks are extended to the captain and crew of the CCGS *Pierre Radisson* for logistical support, C. D. Payne for chemical analyses, P. Larouche for access to satellite and optical data, and M. Roberts, J. Bâcle, and J. Eert for physical data collection and analysis. Special thanks also are due to H. A. Thomsen for valuable discussions and the use of his microscope on board the ship and to D. J. S. Montagnes, E. B. Sherr, W. F. Vincent, and an anonymous reviewer for comments and suggestions.

and retention of particles leading to phytoplankton patchiness (Franks 1995). Fronts associated with interleaving waters could also generate habitats for heterotrophic protists and bacteria that benefit from transparent exopolymeric particles formed under turbulent conditions and subsequently trapped at density interfaces (MacIntyre et al. 1995; Schuster and Herndl 1995). Although interleaved waters persist over time scales relevant to microbial life cycles, their effects on microbial communities have not been explored.

Bacteria and viruses in open waters are dependent on biological carbon fixed in the euphotic zone. Bacterial abundance is generally correlated with phytoplankton biomass (Simon et al. 1992) and has been used as a tracer of water masses (Talpsepp et al. 1999). Heterotrophic bacteria persist in a variety of states from dead to very active (Zweifel and Hagström 1995; Gasol et al. 1999; Barer and Harwood 1999), and the proportion of inactive, damaged, or dead cells varies over time, area, depth, and according to photosynthetic biomass and the presence of bacterial grazers (Gasol et al. 1999). In the same way that bacterial abundance can be useful for tracing water masses, the proportion of healthy versus less healthy bacteria is likely to provide information on the microbial history of a given parcel of water. For example, more bacteria would be expected in regions with high concentrations of utilizable substrates. Furthermore, damaged and dead bacteria would accumulate over time within longer lived areas of resuspension and retention because grazers often discriminate against dead bacteria (González et al. 1993; Boenigk and Arndt 2000). Viruses are closely associated with suitable hosts, and because viruses have both high production and loss rates (Wommack and Colwell 2000), the ephemeral concentration of viruses could also be a useful indicator of water parcel duration.

Protist species composition provides additional clues for tracking the history or persistence of interleaved waters. Ciliates and dinoflagellates often follow diatom blooms (Levinsen et al. 1999) and ciliate patches have been observed in association with intersecting water masses in the Irish Sea (Montagnes et al. 1999). Ciliates are relatively independent of irradiance. If ciliates are cut off from a supply of suitable prey, they quickly die or perhaps form cysts (Montagnes 1996). This implies that ciliates are sensitive to short-term conditions. Thus, the structure and species composition of the protist community, along with the associated bacterial and viral characteristics, could provide evidence as to whether communities within distinct TS layers are part of a bloom that is actively growing and maintained by trapping and retention of surface-produced particles, such as aggregates of phytoplankton and marine snow (MacIntyre et al. 1995), or are simply a community that results from sinking of senescent phytoplankton cells. The existence of retentive TS layers would affect the depth of remineralization of particulate organic matter (POM) and, thus, the biogeochemical dynamics and fate of carbon in the upper ocean.

The North Water Polynya (NOW), a large region of persistent ice-free conditions between Ellesmere Island (Canada) and Greenland, provided an ideal environment to assess the effects of water column interleaving on microbial community structure. Polar seas are typically regarded as systems with well-mixed, unstable surface layers. However, ho-

mogenous density profiles in the NOW region belie a high degree of structure caused by water column interleaving (Melling et al. 2001; Bâcle et al. 2002). Our overall objective in the present study was to examine water columns subjected to different degrees of interleaving and to determine how the physical structure affected microbial populations. We examined vertical community structure and compared phytoplankton and other protists within layered water columns to those in a nonlayered water column. Other characteristics of these communities—such as nutrient levels, the distribution of total bacteria, bacteria with damaged or open membranes, actively respiring bacteria, and viral concentrations—were investigated to identify additional key variables that could be used to characterize the history and persistence of the interleaving waters.

Materials and methods

Physical measurements and field sampling—The NOW (Fig. 1) is an 80,000-km² region of recurrent open water within the ice pack between Ellesmere Island (Canada) and Greenland (longitude 76–79°N and centered at about latitude 75°W). The region was intensively sampled on board the Canadian icebreaker *Pierre Radisson* between April and July 1998 as part of the International North Water Polynya Study. NOW occurs annually after an ice bridge forms across Smith Sound at its northern boundary. Water from under the Arctic Ice Pack flows into Northern Baffin Bay, where it meets Atlantic deep water and other locally modified water masses. Samples for this study were collected in June 1998. Casts were obtained using a Falmouth Scientific Instruments Integrated CTD or SeaBird-25 CTD. Salinity (S) samples for calibration of CTD measurements were analyzed with a Guildline Auto-Sal salinometer. Values of potential temperature (θ) and potential density were computed using the algorithms given in UNESCO (1983).

Six sites were selected to represent the greatest possible range of conditions within the logistical constraints of the overall program (C18, C23, C40, C44, C56, and C72, Fig. 1). Sampling depths were selected while viewing the temperature and salinity traces of the downward CTD casts, and depths were selected to reflect as many conditions as possible down the water column. All stations were sampled between 0630 and 0800 h local time. Five of the sites were sampled at six depths from near surface to 200 m, and one site (C18) at four depths. One additional site (C47) was sampled at 11 and 200 m to verify methods used for bacterial enumeration. In situ optical measurements were made with a Satlantic SeaWiFS profiling multichannel radiometer to estimate the diffuse attenuation coefficients of photosynthetically available radiation (PAR). Water samples were collected using either a rosette sampler (General Oceanics) equipped with 10-liter Niskin-type bottles and the Falmouth Scientific Instruments Integrated CTD or 5-liter Niskin bottles on a line when physical measurements were made using the SeaBird-25 CTD. Autoclaved 2-liter Nalgene polycarbonate bottles were rinsed three times with sample water before filling. All biological analyses were from subsamples of these bottles, which were kept in darkness between 0 and

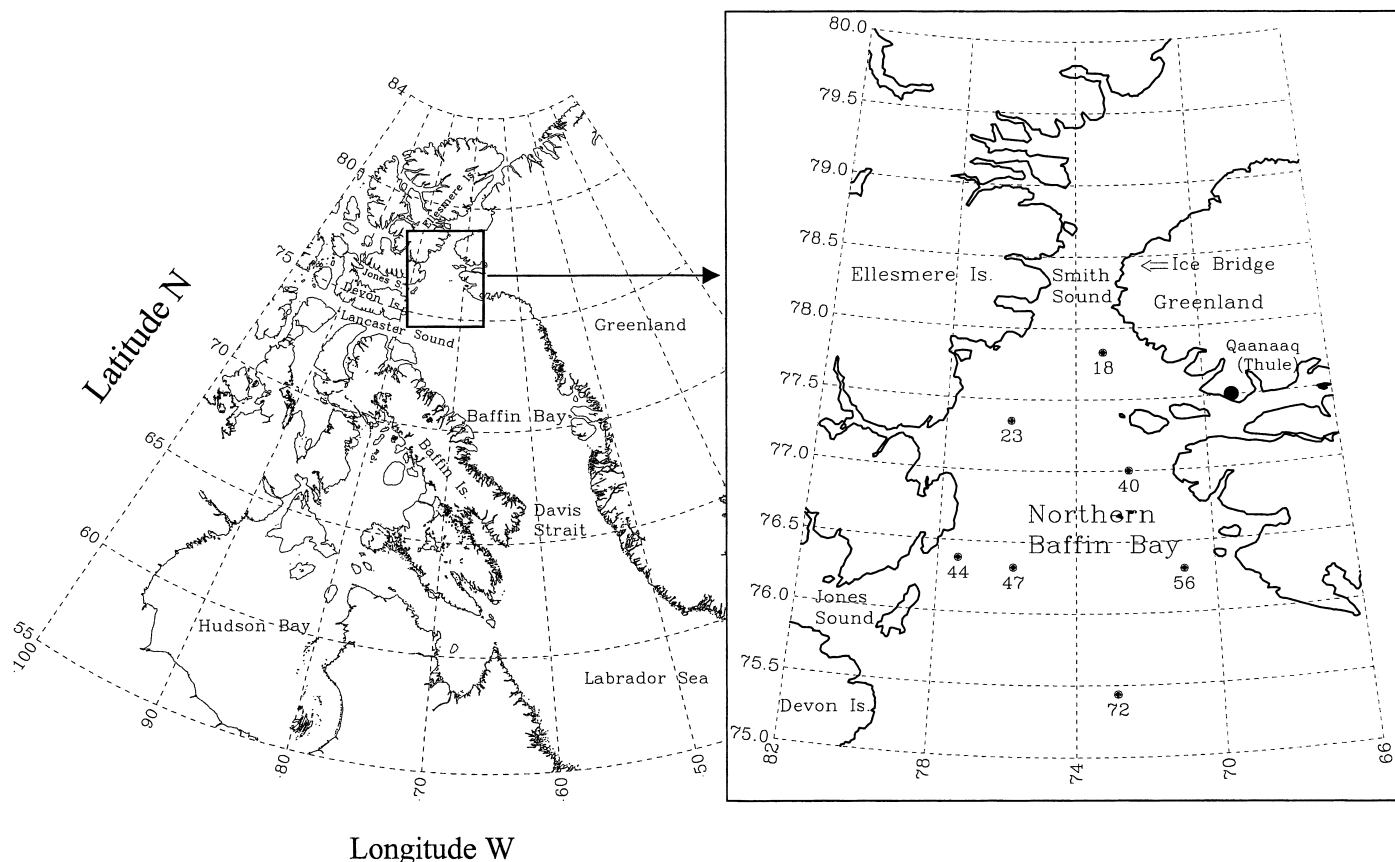


Fig. 1. Map of the North Water Polynya; station numbers are preceded by a "C" in the text. The polynya forms in winter when an ice bridge blocks Smith Sound.

2°C during manipulations. Nutrient samples were taken from Niskin bottles from the same cast. When the rosette was used, water samples were from the same cast as the physical profiles presented here. When a line was used, samples were collected immediately after the CTD profile.

Chemical and biological measurements—Samples for Chl *a* were filtered onto Whatman GF/F filters, which were stored frozen. These were later extracted ashore in boiling ethanol and measured fluorometrically using a Sequoia-Turner model 450 spectrofluorometer (Nusch 1980; Jeffrey and Welschmeyer 1997). Samples for analysis of fluorescent chromophoric dissolved organic matter (FCDOM) were pre-filtered on board the ship using 0.2- μm Sartorius Minisart syringe filters. The filtrate was stored in darkness at 2°C in amber glass bottles until analysis by fluorescent emission scanning over 400–600 nm using an excitation wavelength of 348 nm. Raman units (Ru) were calculated from the 435-nm peak divided by the area under the Raman peak (Determann et al. 1994). Soluble reactive phosphorus (SRP) and nitrate + nitrite (N) were analyzed on board the ship with an ALPKEM autoanalyzer and colorimetric protocols (Grasshoff 1976).

Virus-sized particles (VSP) were estimated using a modification of the Noble and Fuhrman (1998) technique. Samples (1 ml) preserved with a mix of glutaraldehyde and formaldehyde (Tsuji and Yanagita 1981) were filtered onto a

0.02- μm , 25-mm Whatman Anodisc filter and stained using a mixture of SYBR I and SYBR II green (Molecular Probes) fluorescent DNA and RNA markers, respectively (final dilution 4×10^{-3} v/v each). The filters were then mounted between a slide and cover slip using Aquapolymount (Polysciences). The slides were stored flat at 2°C for 24 h and stored frozen until examination by microscopy up to 2 weeks later. The VSP were counted at $\times 1,000$ under epifluorescence using a Zeiss Axiovert 10 microscope equipped with a blue filter block (Zeiss block 4877 09).

For bacterial analysis, subsamples of water were preserved in 2% final concentration EM-grade paraformaldehyde and stored 1–4 weeks before staining with 4',6-diamidino-2-phenylindole (DAPI, 0.0007 v/v) and filtering onto membrane filters (Porter and Feig 1980). Bacteria were counted with a Zeiss Axiovert 10 at $\times 1,000$ and an ultraviolet (UV) filter block (Zeiss 4877 02). Bacteria-sized actively respiring cells (ARCs) were estimated using 5-cyano-2,3 ditolyl tetrazolium chloride (CTC) as in Lovejoy et al. (1996). On board the ship, bacterial abundance was also estimated on freshly collected subsamples (no preservative) after staining with two fluorophores, SYBR green I (SYBR) and SYTOX (Molecular Probes). These two stains both fluoresce green under blue excitation and were compatible with the microscope filter blocks available on board the ship. The bright fluorescence of these two stains also meant that cells were unambiguously counted under difficult conditions.

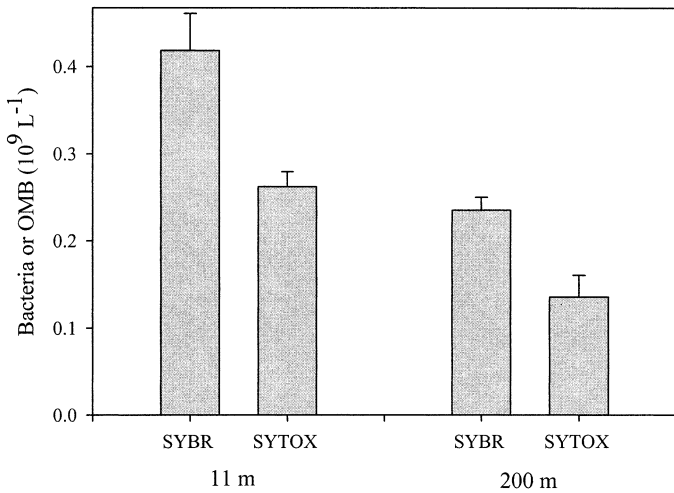


Fig. 2. Initial comparison of SYBR green I (total bacteria) and SYTOX (open-membrane bacteria, OMB) using samples taken from Sta. C47 (see Fig. 1). Samples were taken at 11 m (upper euphotic zone above the halocline) and 200 m. The bars indicate the means of three replicates for the two treatments at the two depths; error bars indicate standard deviations.

SYBR I binds to double-bonded DNA and has cell wall permeability characteristics similar to the more commonly used DAPI and Hoechst 33342 stains, which means that it easily enters both live and dead cells (product information from Molecular Probes). SYTOX is also DNA specific, but it is actively excluded by many bacteria with functional membranes and is used to test for cells with compromised (leaky) membranes. It has been suggested that it is equivalent to the more widely used propidium iodide (product information from Molecular Probes; Roth et al. 1997). These samples for bacteria were stained and mounted on slides within 5 h of collection. All manipulations were done in a laboratory that was always cooler than 8°C. For both SYBR and SYTOX markers, the technique for staining was similar to that used for viruses, with the following modifications: 6 ml of sample was filtered onto 0.2- μ m, 25-mm Whatman Anodisc filters. The filter was floated on a 75- μ l drop (4×10^{-3} dilution) of either SYTOX or SYBR for 15 min, then rinsed by successively placing the filter onto three 70- μ l drops of 0.2- μ m filtered seawater for 5 min each to eliminate unbound dye from the filter surface. The filters were then mounted onto slides using Aquapolymount media. The slides were stored frozen for 24–48 h and counted on board the ship at $\times 1,000$ using an Olympus BH2 fluorescence microscope fitted with an Olympus blue filter block. Between 400 and 800 cells were counted in all cases. At Sta. C47, SYBR and SYTOX stains were compared at two depths using three replicates each. The three replicates were normally distributed (Kolmogorov–Smirnov normality test) with standard errors from 4 to 10% of the means (Fig. 2), which is considered acceptable for this type of data (Duarte et al. 1990). Because total bacteria were more abundant or equal to SYTOX bacteria, we considered SYTOX bacteria as a subpopulation of the total bacteria. SYTOX-stained cells were designated OMB (open-membrane bacteria).

Eukaryotic microbes (phytoplankton, colorless flagellates,

ciliates, and other protists, referred to collectively as protists throughout the remainder of this paper) were counted using a combination of fluorescence, Nomarski optics, and Utermöhl sedimentation (FNU). This method has been found to give excellent agreement with total counts using a membrane method but, in addition, provides detailed taxonomic information (see references in Lovejoy et al. 2002). Samples were immediately preserved in a buffered glutaraldehyde–formaldehyde mixture and kept at 2°C in the dark (Tsuji and Yanagita 1981). For these samples, 45 ml was sedimented for several weeks in 50-ml Corning centrifuge tubes, after which the top 40 ml was carefully removed using a Pasteur pipette. The final 5 ml was placed in a sedimentation chamber with DAPI (0.0007 v/v) and Calcofluor white (0.001 v/v), and resettled for 24 h prior to counting. The DAPI was used to visualize the DNA within the nucleus and Calcofluor to stain cellulose and chitin for quick identification of thecate dinoflagellates and loricate taxa such as *Dinobryon* spp. DAPI and Calcofluor fluoresce slightly different shades of blue under UV excitation (Zeiss Filter block 4877 02). Chl *a* in cells was confirmed under a blue Zeiss filter block (4877 09), and the presence of phycobilin in cryptophytes was verified using a green filter block (Zeiss 4877 15). The samples were counted at $\times 100$, $\times 400$, and $\times 1,000$ with a Zeiss Axiovert 10 or 100 inverted microscope. In deep (100 and 200 m) samples, a total of 125 to 500 cells were counted (except for C40, 200 m, where after 200 fields only 14 individual cells were seen). In the upper water column, 400 to 2,500 cells were counted (except C23, 5 m, where 6,291 cells were seen in 200 fields). Phytoplankton and other protists were identified to the lowest taxonomic level possible using light microscopy (details in Lovejoy et al. 2002). Cell volumes were calculated as in Hillebrand et al. (1999) and carbon contents estimated as in Menden-Deuer and Lessard (2000). To minimize the accumulated error involved in estimating differences between communities, we used biomass C values in our subsequent index, as suggested by Duarte et al. (1990).

To quantify differences in protist community structure down the water column and to compare stations, a ternary community difference (TCD) index was developed. The proportional contribution of the three functional and taxonomically defined protist groups (diatoms, ciliates including tintinnids, and flagellates along with dinoflagellates) to community carbon biomass at each depth was plotted in ternary space. The aim was to identify three mutually exclusive categories that represented varying proportions of eukaryotic biomass within the samples. A ternary plot was made for each station containing N loci (x, y, z), where N is the number of depths sampled at that station. The loci for adjacent depths were joined by straight lines and the cumulative distance between all loci was then determined. This value was divided by the maximum distance possible between all points, $[N - 1] \times 100$, to give a dimensionless TCD index.

$$\text{TCD} = \frac{\sum_{i=2}^{i=N} [(x_i, y_i, z_i) - (x_{i-1}, y_{i-1}, z_{i-1})]}{[N - 1] \times 100}$$

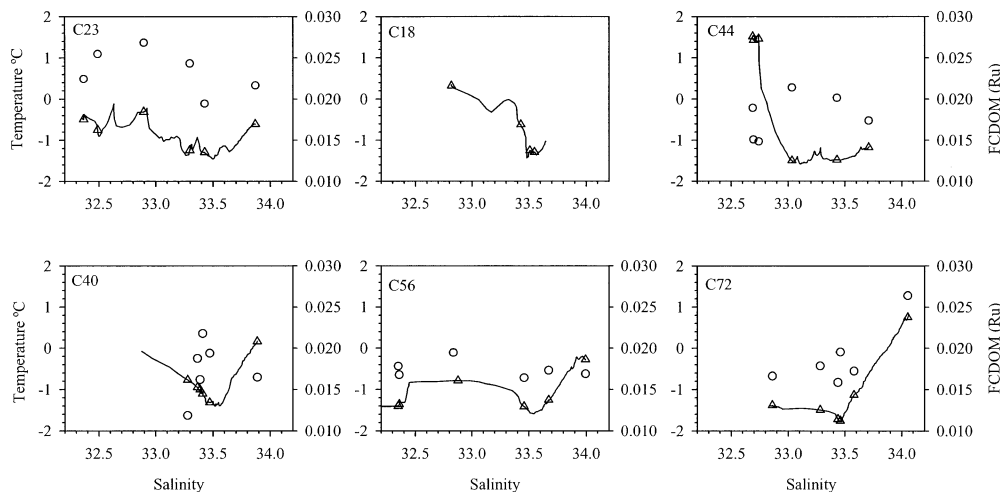


Fig. 3. Lines indicate TS characteristics of the six stations that were intensively sampled (see *text*). The triangles on the TS lines indicate where samples were taken and circles are FCDOM values in Raman units (left axis); no FCDOM data were available for Sta. C18.

An index of physical interleaving (IPI) was calculated by first applying a smoothing filter consisting of a Kaiser–Bessel window with a half-width of 10 m to the raw temperature data from the surface halocline down to a depth of 200 m and then calculating the root mean square difference between this smoothed temperature profile and the raw temperature data.

Results

Physical properties of the water columns—Temperature–salinity diagrams show that the extent of water mass interleaving was variable but could be detected at all stations sampled except C72 (Fig. 3). Stas. C23 and C56 showed some surface freshening (salinities less than 32.5) associated with ice melt. There were anomalies associated with interleaving at other stations in the form of temperature spikes above the base of the polar mixed layer (PML; McLaughlin et al. 1996) located at salinities of ~ 33.6 . Fluorescent chromophoric dissolved organic matter (FCDOM) was another indicator of different waters. The FCDOM concentrations were higher in the northern part of the polynya (Sta. C23) and lowest near the southern regions (Stas. C56 and C72). The FCDOM coefficients of variation within the upper 100 m ($n = 5$) were 20% at Sta. C40, 16% at C44, 12% at C23, 7% at C56, and 8% at C72 (Fig. 3); no FCDOM data were available for Sta. C18.

The depth–temperature profiles also highlight that interleaving was greatest at Sta. C23 and least at C72 (Fig. 4). The depth limit of the euphotic zone, defined as 1% of surface PAR, was near 20 m at Stas. C23, C44, C40, and C18; ~ 37 m for C56; and ~ 47 m for C72. Nutrients were depleted in the upper euphotic zone for all stations except C72 (Fig. 5). Nitrate N was lower than SRP near the surface at Stas. C23, C44, and C56. The nitracline varied from < 19 m (C40) to > 50 m (C23). At Sta. C23, there were slightly higher nutrient concentrations at 16 m compared to 40 m (Fig. 5).

Biological characteristics of the water column—At all stations, Chl *a* concentrations generally decreased down the water column and showed no correlation with protist biomass ($r = 0.48$, $p > 0.05$). Near-surface Chl *a* concentrations were highest overall at Sta. C23, with values of 6.9 and $8.8 \mu\text{g L}^{-1}$ for 5 and 16 m, respectively, and at Sta. C18 with 7.3 and $4.9 \mu\text{g L}^{-1}$ at 10 and 40 m, respectively. Chl *a* concentrations within the euphotic zone at the other stations varied from 1.4 to $3.6 \mu\text{g L}^{-1}$.

Large differences among stations were evident in the protist biomass profiles (Fig. 4). Sta. C23 had peaks and troughs in protist biomass, whereas at Sta. C72, the biomass was greatest near the surface and decreased with depth. The vertical distribution patterns were between these two extremes at the remaining four stations. VSP concentrations (Fig. 6) were higher in the samples from < 100 m compared to the samples from 100 and 200 m, except at Sta. C23 where the value at 100 m was similar to shallower depths. The minimum VSP concentration was at 200 m at C23 (2.07×10^8 VSP L^{-1}), but the lowest average water column concentration of VSP was at Sta. C72. There was no linear relationship between protist biomass and VSP; however, the two variables were significantly correlated (Spearman's rank order coefficient of correlation, $\rho = 0.62$, $p < 0.001$). VSP and bacteria numbers were also correlated ($\rho = 0.64$, $p < 0.001$).

There was a positive relationship between DAPI bacteria and SYBR-stained bacteria ($\rho = 0.75$, $p < 0.001$). The estimates of SYBR bacteria were generally higher than those of DAPI bacteria, and counts from the SYBR treatment are therefore considered as total bacteria (all bacteria-sized particles that contained sufficient DNA to be stained) throughout the rest of this paper. At Sta. C47, SYBR and SYTOX stains were compared at two depths using three replicates each (Fig. 2). There were significant depth and stain effects (two-way ANOVA, $p < 0.001$, for both variables). SYTOX stained cells were designated OMB.

The relative duration of bacterial activity was inferred

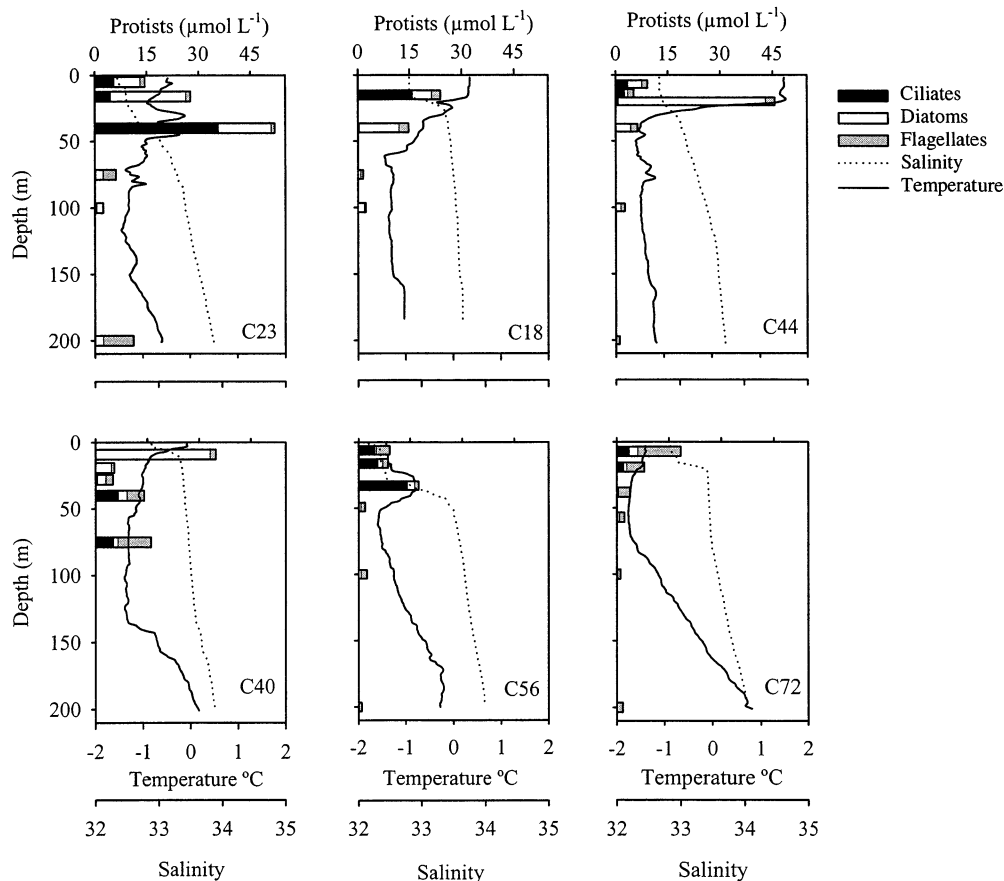


Fig. 4. Protist biomass at the six intensively sampled stations. The stacked bars indicate protist biomass C ($\mu\text{mol C L}^{-1}$) for the three groupings used for the TCD index (see text).

from the minimum numbers of total bacteria and OMB. The lower concentration of bacteria-sized particles in most marine surface waters is $\sim 2.5 \times 10^5 \text{ ml}^{-1}$ (Shimeta 1993). Populations were considered “relics” in samples where both OMB and bacterial concentrations were below this limit. Total bacterial and OMB concentrations greater than this minimum value indicated a water mass with current or recent production. Assuming that at least a fraction of OMB resulted from grazing or viral lysis, concentrations of bacteria greater than those of OMB were interpreted as situations in which bacterial production exceeded losses. Bacterial abundance (Fig. 7) varied among stations and with depth. Within the upper 100 m, bacterial concentrations were greatest at Sta. C23, with average integrated values of $1.42 \times 10^9 \text{ cells L}^{-1}$, and least at C72, with an average integrated value $< 0.2 \times 10^9 \text{ cells L}^{-1}$. There was also greater variability with depth at Sta. C23 compared to C72. The other four stations were between these two extremes. At all stations, minimum total bacterial abundances occurred at 200 m.

The concentrations of OMB (Fig. 7) also varied considerably with depth at all stations except C72. The greatest OMB concentrations were from Sta. C23, with an average integrated concentration in the upper 100 m of $0.69 \times 10^9 \text{ cells L}^{-1}$. At Sta. C72, OMB closely matched total bacteria and averaged $< 0.2 \times 10^9 \text{ L}^{-1}$ at 38, 57, and 100 m. OMB

concentrations at the remaining stations fell between these two extremes. The average concentrations of bacteria and OMB ($0.19 \times 10^9 \text{ L}^{-1}$) at Sta. C72 were used to define the threshold bacterial concentration in the studied system; that is, the residual concentration corresponding to a low probability of encounters with grazers and viruses (Shimeta 1993).

Actively respiring cells (ARCs, i.e., bacteria that converted CTC to a fluorescent product) were determined at four stations. Both the numbers and proportions of ARCs to total bacteria were low at these stations. The highest proportions recorded were 3.0–4.5% at Sta. C56, with 1.3–2.3% at C40, 0.3–0.4% at C44, and 0.7–1.4% at C72. The lowest values at all stations were in deepest waters.

Biomass peaks and dominant taxonomic groups—The depth of maximum protist biomass (B_{max}) varied among stations. B_{max} was located in the upper 10 m at Stas. C18, C40, and C72 and was deeper at Stas. C23 (40 m), C56 (33 m), and C44 (20 m). At Sta. C72, heterotrophic flagellates and small (~ 10 – $20 \mu\text{m}$ diameter) chlorophyll-containing gymnodinoid dinoflagellates were the biomass dominants. At the other stations, peak biomass corresponded to either diatoms or ciliates (Fig. 4). At Stas. C23, C40, and C56, ciliate biomass peaked below depths of low biomass. At Stas. C23 and C40, large (60 – $70 \mu\text{m}$) heterotrophic naked gymnodinoid

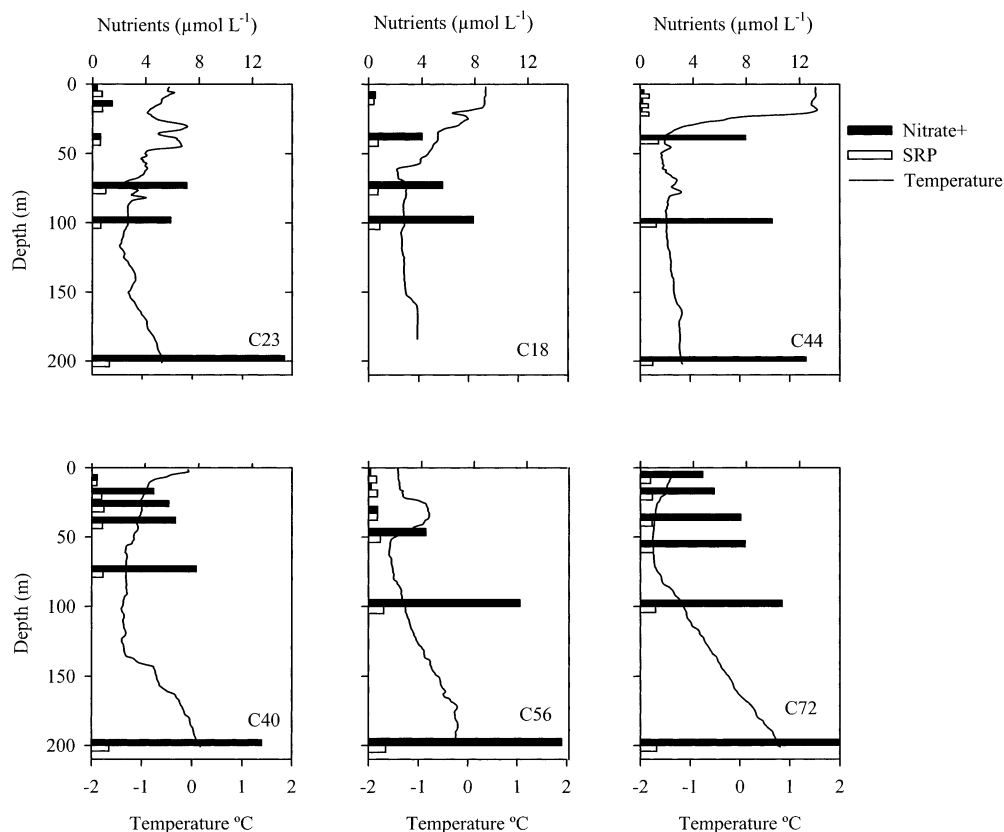


Fig. 5. Nutrient profiles ($\mu\text{mol L}^{-1}$) at the six intensively sampled stations. Upper dark bars indicate N (nitrate + nitrite), and lower white bars indicate SRP (soluble reactive phosphorus). The relative extent of interleaving can be seen by the temperature profiles.

dinoflagellates [*Gymnodinium gracile* Bergh, *Gyrodinium lachryma* (Meunier) Kofoid et Swezy, *Gyrodinium pepo* (Schütt) Kofoid et Swezy, and similar species] were biomass dominants at 75 m. The protist communities in most of the other samples were dominated by diatoms; in particular *Thalassiosira* spp., most commonly *T. antarctica* var. *borealis* G. Fryxell, Douchett et Q. Hubbard and *T. hyalina* (Grunow) Gran.

Synthesis—The lowest value for the protist community index TCD was at Sta. C72 (Fig. 8A), and the highest was at Sta. C23 (Fig. 8B). For the full set of stations, TCD was a close linear function of the IPI (Fig. 8C). The greatest interleaving was at Sta. C23, which showed 12 distinct layers and had the highest IPI. The lowest IPI was from the southernmost station (C72). The remaining stations showed various degrees of water mass interleaving and TCD. Overall, the two indexes were strongly correlated ($r = 0.984$; $p < 0.001$; Fig. 8C).

There was also a significant linear correlation between the IPI and integrated concentrations in the upper 100 m for OMB ($r = 0.81$, $p < 0.05$, $n = 6$) and VSP ($r = 0.91$, $p < 0.001$, $n = 6$), but not for total bacteria ($r = 0.79$, $p = 0.053$, $n = 5$). Total bacteria were only estimated at three depths for Sta. C18; that station was not included in the analysis.

To analyze water column structure in greater detail, we

classified each sample from all six stations into five broad “bloom state” categories based on relative protist and bacteria biomass, nutrient levels, and the dominant protist (Table 1). The prebloom (category 1) was characterized by low protist biomass and high nutrients. Samples from <100 m at Sta. C72 made up this group. Taxonomically, flagellates, including the enigmatic heterotrophic flagellate *Ebriia* sp., accounted for the greatest proportion of the total biomass. In the late to postbloom near surface (category 2), nutrients were depleted. In this category, the protist biomass near the surface and away from the halocline was dominated by ciliates, including the tintinnid genera *Parafavella*, *Ptychocylics*, and *Coxliella* or the naked oligotrich *Strobilidium* sp.; just above the halocline the protist biomass was dominated by diatoms, especially *Thalassiosira* spp. and *Coscinodiscus* spp. Below the euphotic zone (category 3), possibly sinking communities were identified by predominantly phototrophic protist biomass and high nutrients. Diatoms were mostly the same species as those within the euphotic zone, but chains and colonies of *Thalassiosira* spp., *Chaetoceros* spp., and ribbon-forming *Navicula* spp. contained fewer cells, and the overall protist biomass was low ($<6.2 \mu\text{mol C L}^{-1}$). Sta. C56 at 49 m depth was exceptional in having the coccolithophorid *Coccolithus* sp. as the dominant protist. Heterotrophic protist communities near the bottom of or below the euphotic zone (category 4) were dominated by blooms of either ciliates or large dinoflagellates, with variable nutrient

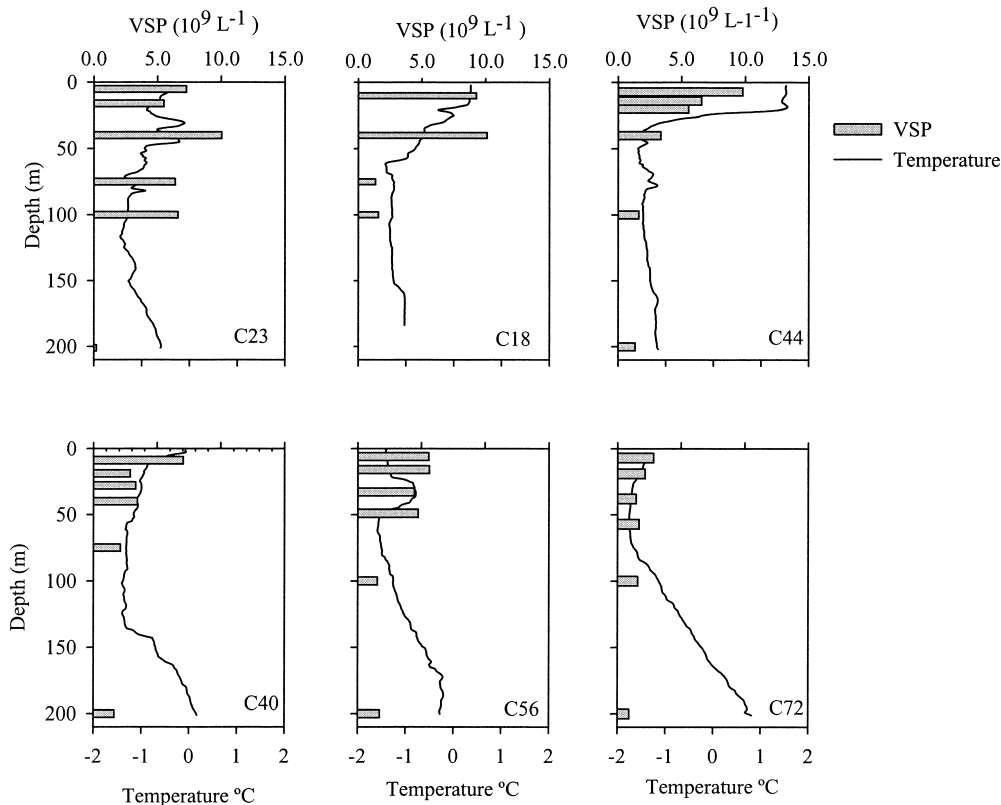


Fig. 6. Profiles of VSP (virus-sized particles) at the six intensively sampled stations. Bars indicate VSP L^{-1} .

concentrations. Deep communities below the PML (category 5) had high nutrients and low protist biomass. Within these five categories, category 1 and some deep samples within category 5 had bacterial and OMB concentrations at or below $\sim 0.19 \times 10^9$ cells L^{-1} . Bacterial concentrations were greater than this threshold for all other samples. VSP concentrations were higher in categories 2, 3, and 4 compared to categories 1 and 5.

Discussion

Physical interleaving—Five of the six stations sampled had TS profiles consistent with interleaving water masses above the lower boundary of the PML. The bottom of the PML is located at the minimum-temperature, 33.6 salinity knee and was most evident for Stas. C40 and C72 (Fig. 3). Waters enter the NOW polynya from either the Arctic Ocean via Smith and Jones Sound (Fig. 1) or from the West Greenland Current after originating in Southern Baffin Bay and the Labrador Sea. These two sources are considered “assemblies” consisting of the PML (70–100 m depth, and salinities >33.6) and one or two deeper layers separated by deeper haloclines. The northern assembly (NA, from the Arctic) and the southern assembly (SA, from Southern Baffin Bay and Labrador) combine to form the North Water assembly (NWA). The NWA can be subgrouped by the relative contributions of the SA and NA as thermohaline intrusions (details in Bâcle et al. 2002). There were intrusions within the

PML above the permanent pycnocline at all stations except the southernmost (C72, Fig. 3) that were uniquely SA water (Bâcle et al. 2002). The IPI confirmed that Sta. C72 was not influenced by these intrusions. Stas. C40 and C56 on the eastern side of the polynya were less affected compared to Sta. C18 near Smith Sound or C44 near Jones Sound (Figs. 1, 8). Sta. C23 showed the greatest interleaving (highest IPI), possibly because of Arctic inflows via both Smith and Jones Sounds (Melling et al. 2001).

In addition to TS characteristics, the larger coefficients of variation in FCDOM at Stas. C23, C44, and C40 (Fig. 3) suggest layers from different source waters. In April, NA waters had FCDOM values of ~ 0.04 Ru compared to Baffin Bay samples that all had values < 0.02 Ru (Lovejoy unpubl. data). The low coefficients of variation for FCDOM at Stas. C72 and C56 suggest similar source waters in the upper 100 m at these two stations. The larger FCDOM coefficients of variation at the other three stations indicate either different source waters or photobleaching followed by entrainment below the euphotic zone. Between April and June 1998, Scully and Miller (2000) also found that CDOM, measured spectrophotometrically, tended to be higher at northerly stations below the ice bridge near Smith Sound compared to more southerly stations within the NOW Polynya. They also noted that, although CDOM in the NOW region could have been affected by photobleaching, it was considerably less than in more temperate waters.

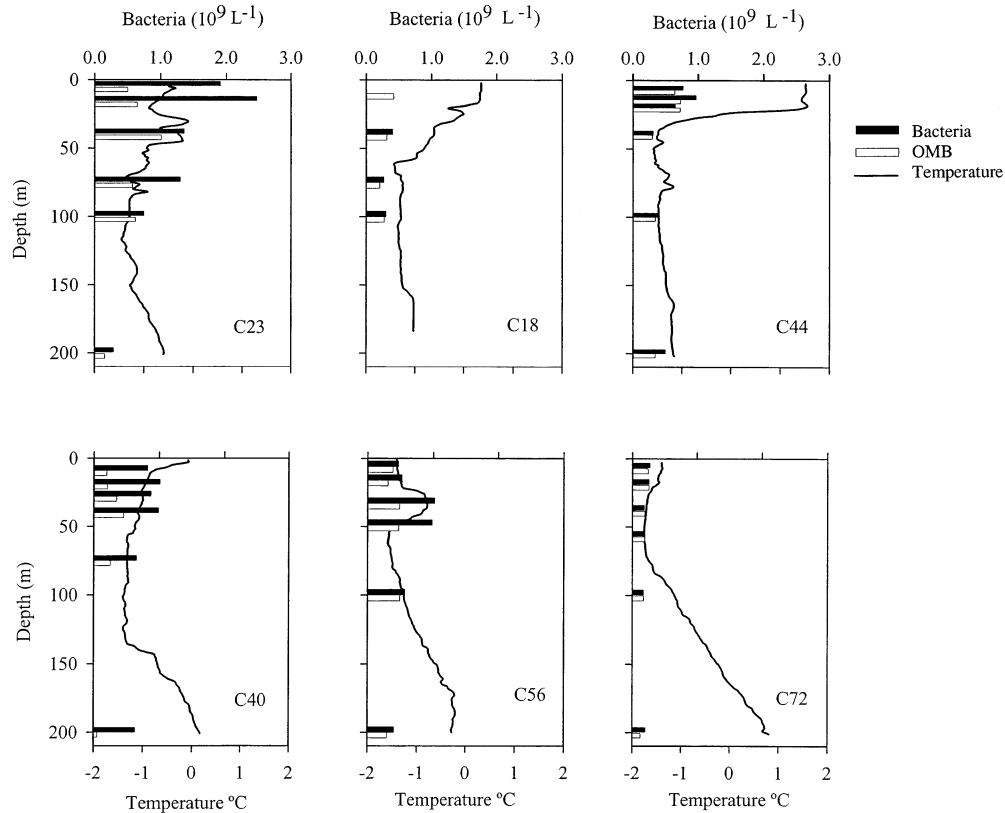


Fig. 7. Profiles of bacteria (dark bars) and OMB (open-membrane bacteria, white bars) at the six intensively sampled stations (cells L^{-1}). The relative extent of interleaving can be seen by the temperature profiles.

Bacterial and viral distributions—The reliability of counts using two bright green SYBR and SYTOX dyes was within the error range usually found with microscopic counts using DAPI or Acridine Orange (Gasol et al. 1999). The two newer stains did fade rapidly using our mounting media and protocol, and the addition of an antifading compound or use of a flow cytometer would probably yield a lower coefficient of variation. We estimated OMB using the membrane-impermeant fluorophore SYTOX green, which reportedly has

properties similar to propidium iodide (Roth et al. 1997). These two dyes are considered markers for dead bacteria because they are actively excluded by functional membranes in common laboratory bacterial strains. In contrast, DAPI and SYBR green I are membrane permeant and stain all bacteria. The use of impermeant and permeant dyes is the basis for commercially available viability kits (e.g., Molecular Probes, Boulos et al. 1999). Although these viability tests work with laboratory strains and under laboratory con-

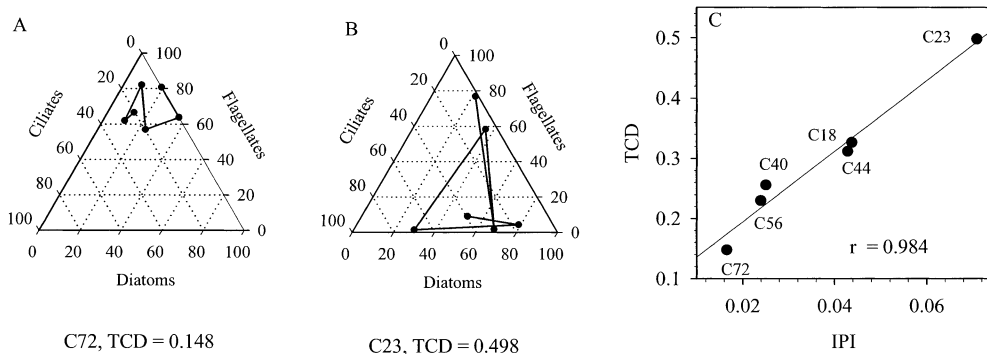


Fig. 8. Application of the ternary community difference index (TCD). All members of the protist community were classified as either flagellates (including dinoflagellates), diatoms, or ciliates (see text for details). The index is illustrated for Stas. (A) C72 and (B) C23. Panel C shows the relationship between TCD and the index of physical interleaving (IPI; see text). The line in panel C is calculated using type II regression.

Table 1. Bloom state classification as described in the text. A low ratio (<8 , from deep waters) of N:P ($\mu\text{mol L}^{-1}$) indicates drawdown of N relative to P. The accumulation of OMB (OMB accum.) indicates open membrane bacteria concentrations $>0.20 \times 10^9 \text{ L}^{-1}$ (Y) or $<0.15 \times 10^9 \text{ L}^{-1}$ (N). Regions of active bacterial production (Bact. prod.) were assumed if the concentration of total bacteria was greater than $0.20 \times 10^9 \text{ L}^{-1}$ (+); concentrations less than this value are indicated by (-). Data were not available (na) for Sta. C18 in the upper 10 m. Samples are listed by station (depth, m, in parentheses).

Category*	(N:P)	OMB accum.	Bact. prod.	Dominant protist taxa	Samples
1	6.1–8.5	Y	+	<i>Ebriia</i>	C72(7, 19, 38, 57)
2	0.4	Y	+	<i>Parafavella</i>	C23(5)
	1.9	Y	+	<i>Thalassiosira</i>	C23(16)
	1.1	N	+	<i>Coscinodiscus</i>	C40(9)
	0.3	N	+	<i>Ptychocylis</i>	C56(6)
	1.0	Y	+	<i>Coxiella</i>	C56(16)
	0.3–0.4	Y	+	<i>Strobilidium</i>	C44(7–14)
	0.2	Y	+	<i>Thalassiosira</i>	C44(20)
	1.3	Y	na	<i>Strombidium</i>	C18(10)
	9.4	Y	+	<i>Thalassiosira</i>	C23(100)
	6.4	N	+	<i>Thalassiosira</i>	C40(19)
3	6.5	N	+	<i>Thalassiosira</i>	C40(28)
	4.8	Y	+	<i>Coccolithus</i>	C56(49)
	10.0	Y	+	<i>Chaetoceros</i>	C56(100)
	5.8–8.2	N	+	<i>Coscinodiscus</i>	C44(40, 100)
	5.5	Y	+	<i>Thalassiosira</i>	C18(40)
	7.8–9.4	N	+	<i>Navicula</i>	C18(75,100)
	1.03	Y	+	<i>Strombidium</i>	C23(40)
	7.2	Y	+	<i>Gymnodinium</i>	C23(75)
	7.8	Y	+	<i>Strobilidium</i>	C40(40)
	9.3	N	+	<i>Gyrodinium</i>	C40(75)
4	1.0	Y	+	<i>Strombidium</i>	C56(33)
	11.3	L	+	<i>Strombidium</i>	C23(200)
	9.6	L	+	<i>Chrysochromulina</i>	C40(200)
	11.3	N	-	<i>Gymnodinium</i>	C56(200)
	13.4	N	-	<i>Gyrodinium</i>	C44(200)
	8.1–9.5	L	-	<i>Protoceratium</i>	C72(100, 200)

* Categories are 1, prebloom; 2, late bloom; 3, sinking communities below the euphotic zone; 4, subsurface bloom of heterotrophic protists; 5, below the PML with salinities >33.6 .

ditions, in natural mixed assemblages the dyes do not distinguish between truly dead cells with remnant nucleic acids and viable cells with leaky or open membranes (Barer and Harwood 1999). Cells stained with impermeant fluorophores, such as SYTOX, could be in any number of different states including phage-eviscerated bacteria, bacteria damaged but not completely digested by grazers (Hahn and Hofle 1999), and live bacteria that have relatively large open membranes and are not sensitive to particular membrane permeability tests (Gasol et al. 1999). Protist grazing damage and viral impact are consistent with electron microscopy observations that a large percentage (up to 70% in inshore marine waters) of natural marine bacteria lack capsular material and have slight to severely damaged membranes (Heissenberger et al. 1996). However, OMB populations are probably not entirely composed of damaged bacteria, since bacteria living under low-substrate conditions are able to adjust their membrane permeability and can change membrane characteristics by inducing large porins (channels in the outer membrane that allow small molecules to pass freely into the periplasm; see p. 391, White 2000). Therefore, some OMB could be the result of adjustment to starvation stress in bacterial populations.

Over most of the sampling area, bacterial and viral concentrations tended to be low compared to temperate regions (Cochlan et al. 1993), with minimum concentrations at Sta. C72. Overlying ice had cleared less than 24 h prior to sampling this station (P. Larouche, unpubl. satellite data) and all other variables indicated that Sta. C72 was in a prebloom state with high nutrients (Fig. 5) and low protist biomass. Bacterial concentrations at Sta. C72 were near reported grazer threshold levels ($<2.0 \times 10^8 \text{ L}^{-1}$; Shimeta 1993), and interestingly, virtually the entire population had open membranes (OMB).

At the remaining five stations, nutrients were depleted in the surface following the diatom bloom that had started 2 to 4 weeks earlier (Mei et al. 2002). Bacterial concentrations were greater than at Sta. C72 but did not decrease smoothly down the water column as sometimes noted in other studies (Cochlan et al. 1993; Tarran et al. 2001).

Open-membrane bacteria were a subset of total bacteria and the proportion varied considerably among stations and depths. Concentrations were usually greater than the threshold levels for grazers of $\sim 0.2 \times 10^9 \text{ L}^{-1}$ (Shimeta 1993) except at 200 m for Stas. C23, C40, and C72, where they were extremely low ($<0.15 \times 10^9 \text{ L}^{-1}$). This might have

been a consequence of bacteria being in a genuine resting state, which would result in a resistant membrane (Barer and Harwood 1999) that is better able to exclude SYTOX compared to populations nearer the surface.

Choi et al. (1999) have referred to ARCs as “super-active bacteria.” With our limited sampling, we found no clear relationships between these bacteria that reduced CTC and other biological or water column characteristics, except that their proportional contribution to total bacteria decreased with depth as found elsewhere (Sherr et al. 1999). There were no significant correlations between concentrations of ARCs and either total bacteria or OMB. The proportion of CTC-active bacteria is often strongly correlated to bacterial production (Sherr et al. 1999); however, we did not measure this directly and the low proportion of ARCs implies few super-active bacteria were present at the time of sampling.

There were differences in the concentrations of total bacteria and OMB among stations and within the water column at all stations except C72. Overlying photosynthetic production can strongly influence deeper bacterial concentrations (Cochlan et al. 1993). The low total bacterial concentrations at Sta. C72 compared to the other stations, in combination with high concentrations of nutrients and low protist biomass, are consistent with a prebloom state. The low bacterial and OMB concentrations at Sta. C72 represented a prebloom baseline condition in the NOW region. The other five stations sampled had higher bacterial concentrations, which resulted from bacterial growth fueled by an ongoing bloom (Lovejoy et al. 2002; Mei et al. 2002). At least some of the greater-than-baseline OMB concentrations were likely to have been a consequence of bacterial damage that accumulated over time. For the five stations showing water mass interleaving, bacterial and OMB distribution down the water column was not a smooth function of depth but showed a discontinuous distribution that is consistent with water column interleaving.

Middelboe et al. (2002) found that bacterial and viral production were closely coupled in the NOW polynya during July 1998 and that bacterial production was highly dependent on substrate supply. In our study conducted in June, we noted that VSP and bacterial concentrations were correlated, as were VSP and protist biomass. VSP concentrations at Sta. C72 were low compared to other stations and decreased with depth, tracking protist biomass (Figs. 4, 6). However, neither protist biomass nor depth fully explained the variability in VSP distributions among the rest of the stations. For example, VSP concentrations were higher near the surface and decreased with depth in the highly stratified waters of Sta. C44, but at this station, protist biomass was lower at 7 and 14 m compared to 20 m (Figs. 4, 6). This depth distribution pattern suggests a lag between the earlier surface diatom bloom (Mei et al. 2002) and maximum VSP concentrations.

Protist communities—Five distinct communities were identified at the different depths and stations (Table 1). A prebloom community consisting primarily of flagellates and a small number of diatom taxa was confined to Sta. C72 (Figs. 4, 8B). Bacterial and viral concentrations were low. Over the rest of the region, a bloom had begun in early May on the eastern side of the polynya and, later that month, over

the western portion (Bélanger et al. in press). Late-bloom surface communities (category 2) were evident at the five stations. Ciliate–diatom communities near the surface are typical of late-bloom seasonal polar waters (Levinsen et al. 1999). Within the upper water column, ciliates made up a greater proportion of the biomass closer to the surface, whereas diatoms dominated at the halocline (e.g., Stas. C44 and C40; Fig. 4, Table 1).

Between the surface halocline and the top of the PML, two functionally and taxonomically different protist communities were identified (categories 3 and 4, Table 1). Category 3 was below the euphotic zone, primarily dominated by single cells or short chains of *Thalassiosira* spp. and other diatoms that had been responsible for much of the bloom since May (Lovejoy et al. 2002). OMB and bacterial concentrations indicated that substantial bacterial production had recently occurred at these depths. The greater number of VSPs was also indicative of biological activity. This coupling of large sinking cells, bacteria and viruses below the euphotic zone is evidence that particles were sinking sufficiently slowly to provide substrate for free-living bacteria in the water column. Nearly one third of the total samples examined in this study were indicative of a sinking community (category 3, Table 1).

Distinct heterotrophic protist communities were identified between the surface halocline and the bottom of the PML (category 4). Ciliate peaks were identified at Stas. C23, C40, and C56. A second type of heterotrophic protist community dominated by large gymnodinoid dinoflagellates was also noted at Stas. C23 and C40. These few data suggest that ciliates, which feed primarily on small flagellates (Montagnes 1996), were favored higher in the water column compared to the dinoflagellates. The ability of heterotrophic dinoflagellates to persist in the deeper waters as well (category 5) is consistent with the opportunistic nature and trophic diversity of these protists (Lessard 1991).

Biological and physical interleaving—In the NOW, small flagellates were nearly always present at low biomass levels that varied little within the water column (Lovejoy et al. 2002). To obtain a simple index, we chose to group flagellates with dinoflagellates. This grouping was somewhat arbitrary because dinoflagellates are not closely related to other flagellates. Other groupings using more closely related evolutionary and functional categories were possible. For example, ciliates and dinoflagellates are both alveolates, and an alveolate-flagellate-diatom trio might have been a more natural grouping. However, within any one sample taken in the NOW, either dinoflagellates or ciliates tended to dominate, and the greater biomass of ciliates and dinoflagellates made them good counterpoints to the more frequently dominant diatoms. The resulting TCD index using ciliate, diatom, and combined flagellate and dinoflagellate biomass provided a convenient means to quantify the relative contribution of functionally and taxonomically distinct communities to the total protist biomass. Communities at Sta. C72 were similar at all depths, resulting in a low TCD score (Fig. 8A). At the opposite extreme, Sta. C23 had varied communities that were interspersed, resulting in greater distances and crossed lines on the graph (Fig. 8B) because of alter-

nating dominance down the water column by flagellates, ciliates, and diatoms. The most complex water column in terms of physical interleaving also was at Sta. C23. The close correlation between values of TCD and IPI supports the notion that physical interleaving has a direct effect on the biological communities. In general, more complex physical structure was associated with discrete layers dominated by different protists, as well as higher concentrations of VSP, OMB, and, at times, total bacteria.

In contrast to classic spring blooms, with a succession of species starting with large diatoms and moving to small flagellates (<10 μm), the ciliate blooms in the NOW resulted in large organisms (>20 μm) persisting as dominants over an extended period, despite nutrient exhaustion in surface waters (Lovejoy et al. 2002). In this study, we found ciliate biomass peaks both near the surface and below the euphotic zone, implying favorable conditions for ciliates later in the bloom. The net sinking rates of phytoplankton such as diatoms is affected by density differences according to Stokes law and also by changes in vertical and horizontal diffusivity at density interfaces (Lande and Wood 1987). For example, sinking rates can change abruptly at the base of the surface mixed layer, which would account for the large diatom peaks at 20 m at Sta. C44 and 9 m at Sta. C40. Below the surface halocline, the abrupt density differences where interleaving waters meet would favor particle entrapment. The trapped particles would provide sufficient substrate for a complex microbial food web to develop, supporting the ciliates and large heterotrophic naked gymnodinoids (our category 4 communities, Table 1). Interspersed with the depths of particle entrapment were low-biomass communities (category 3). These were dominated by sinking diatoms that are likely to fuel bacterial production in the deep-water column.

Shallow sediment trap studies in the NOW region show that the downward flux of particles decreases rapidly between 50 and 100 m (Huston and Deming 2002). Hargrave et al. (2002) also noted that regions with greatest surface photosynthetic productivity in the NOW had relatively low particle fluxes as determined from moored sediment traps below 300 m. These authors speculated that local production might have been advected out of the region. However, part of this difference could have been because particles were trapped in the upper 100 m, fueling ciliate production in regions of TS interleaving, which tended to coincide with the regions of persistent, high, surface Chl *a* (Bélanger et al. in press). The subsurface concentrations of protists that we found were associated with physically distinct layers; these communities would be well placed to recycle biogenic carbon above the strong permanent pycnocline, prolonging the residence time of nutrients and carbon in the upper reaches of the water column.

Our study provides evidence of pronounced vertical patchiness in heterotrophic and phototrophic communities in a region of the world ocean typically thought of as well-mixed and vertically homogeneous. The close relationship we observed between TCD and IPI implies that water mass interleaving is an important mechanism of physical-biotic coupling. This physical process appears to be common in other regions such as tidal fronts and eddies (Montagnes et al. 1999; Tarran et al. 2001) and might be a widespread mech-

anism of control on microbial biodiversity, community structure and vertical segmentation of biogeochemical processes in the sea.

References

- BÂCLE, J., E. C. CARMACK, AND R. G. INGRAM. 2002. Water column structure and circulation under the North Water during spring transition: April–July 1998. *Deep-Sea Res. II* **49**: 4907–4925.
- BARER, M. R., AND C. R. HARWOOD. 1999. Bacterial viability and culturability, p. 93–137. *In* R. K. Poole [ed.], *Advances in microbial physiology*, v. 41. Academic Press.
- BARTH, J. A., T. J. COWLES, AND S. D. PIERCE. 2001. Mesoscale physical and bio-optical structure of the Antarctic Polar Front near 170° W during austral spring. *J. Geophys. Res.* **106**: 13,879–13,902.
- BÉLANGER, S., AND OTHERS. In press. Phytoplankton dynamics in the North Water Polynya studied during the summers of 1998–2000 using Sea WiFS Imagery. *J. Geophys. Res.*
- BOENIGK, J., AND H. ARNDT. 2000. Particle handling during interception feeding by four species of heterotrophic nanoflagellates. *J. Eukaryot. Microbiol.* **47**: 350–358.
- BOULOS, L., M. PRÉVOST, B. BARBEAU, J. COALLIER, AND R. DESJARDINS. 1999. LIVE/DEAD® *BacLight*™: Application of a new rapid staining method for direct enumeration of viable and total bacteria in drinking water. *J. Microbiol. Methods* **37**: 77–86.
- COCHLAN, W. P., J. WIKNER, G. F. STEWARD, D. C. SMITH, AND F. AZAM. 1993. Spatial distribution of viruses, bacteria and chlorophyll *a* in neritic, oceanic and estuarine environments. *Mar. Ecol. Prog. Ser.* **92**: 77–87.
- CHOI, J. W., B. F. SHERR, AND E. B. SHERR. 1999. Dead or alive? A large fraction of ETS-inactive marine bacterioplankton cells, as assessed by reduction of CTC can become ETS active with incubation and substrate addition. *Aquat. Microb. Ecol.* **18**: 105–115.
- DETERMANN, S., R. REUTER, P. WAGNER, AND R. WILLKOMM. 1994. Fluorescent matter in the eastern Atlantic Ocean Part 1: Method of measurement and near-surface distribution. *Deep-Sea Res. I* **41**: 659–675.
- DUARTE, C. M., C. MARRASÉ, D. VAQUÉ, AND M. ESTRADA. 1990. Counting error and the quantitative analysis of phytoplankton communities. *J. Plankton Res.* **12**: 295–304.
- FRANKS, P. J. S. 1995. Thin layers of phytoplankton: A model of formation by near-inertial wave shear. *Deep-Sea Res. I* **42**: 75–91.
- GASOL, J. M., U. L. ZWEIFEL, F. PETERS, J. A. FUHRMAN, AND Å. HAGSTRÖM. 1999. Significance of size and nucleic acid content heterogeneity as measured by flow cytometry in natural planktonic bacteria. *Appl. Environ. Microbiol.* **65**: 4475–4483.
- GONZÁLEZ, J. M., E. B. SHERR, AND B. F. SHERR. 1993. Differential feeding by marine flagellates on growing versus starving, and on motile versus nonmotile, bacterial prey. *Mar. Ecol. Prog. Ser.* **102**: 257–267.
- GRASSHOFF, K. 1976. *Methods of seawater analyses*. Weinheim.
- HAHN, M. W., AND M. G. HOFLE. 1999. Flagellate predation on a bacterial model community: Interplay of size-selective grazing, specific bacterial cell size, and bacterial community composition. *Appl. Environ. Microbiol.* **65**: 4863–4872.
- HARGRAVE, B. T., I. D. WALSH, AND D. W. MURRAY. 2002. Seasonal and spatial patterns in mass and organic matter sedimentation in the North Water. *Deep-Sea Res. II* **49**: 5227–5244.
- HEISSENBERGER, A., G. G. LEPPARD, AND G. J. HERNDL. 1996. Relationship between the intracellular integrity and the morphol-

- ogy of the capsular envelope in attached and free-living marine bacteria. *Appl. Environ. Microbiol.* **62**: 4521–4528.
- HILLEBRAND, H., C.-D. DÜRSELEN, D. KIRSCHTEL, U. POLLINGER, AND T. ZOHARY. 1999. Biovolume calculation for pelagic and benthic microalgae. *J. Phycol.* **35**: 403–424.
- HUSTON, A. L., AND J. W. DEMING. 2002. Relationships between microbial extracellular enzymatic activity and suspended and sinking particulate organic matter: seasonal transformations in the North Water. *Deep-Sea Res. II* **49**: 5211–5225.
- JEFFREY, S. W., AND N. A. WELSCHMEYER. 1997. Spectrophotometric and fluorometric equations in common use in oceanography, p. 597–615. *In* S. W. Jeffery, R. F. C. Mantoura, and S. W. Wright [eds.], *Phytoplankton pigments in oceanography*. Monographs on Oceanographic Methodology. SCOR UNESCO.
- LAL, D., AND T. LEE. 1988. Cosmogenic ^{32}P and super ^{33}P used as tracers to study phosphorus recycling in the upper ocean. *Nature* **333**: 752–754.
- LANDE, R., AND A. M. WOOD. 1987. Suspension times of particles in the upper ocean. *Deep-Sea Res. IA* **34**: 61–72.
- LESSARD, E. J. 1991. The trophic role of heterotrophic dinoflagellates in diverse marine environments. *Mar. Microb. Food Webs* **5**: 49–58.
- LEVINSEN, H., T. G. NIELSEN, AND B. W. HANSEN. 1999. Plankton community structure and carbon cycling on the western coast of Greenland during the stratified summer situation. II. Heterotrophic dinoflagellates and ciliates. *Aquat. Microb. Ecol.* **16**: 217–232.
- LOVEJOY, C., L. LEGENDRE, B. KLEIN, J.-É. TREMBLAY, R. G. INGRAM, AND J.-C. THERRIault. 1996. Bacterial activity during early winter mixing (Gulf of St. Lawrence, Canada). *Aquat. Microb. Ecol.* **10**: 1–13.
- , ———, M.-J. MARTINEAU, J. BÂCLE, AND C. H. VON QUILLFELDT. 2002. Distribution of phytoplankton and other protists in the North Water. *Deep Sea Res. II* **49**: 5027–5047.
- MACINTYRE, S., A. L. ALLDREDGE, AND C. C. GOTSCHALK. 1995. Accumulation of marine snow at density discontinuities in the water column. *Limnol. Oceanogr.* **40**: 449–468.
- MAY, B. D., AND D. E. KELLEY. 2001. Growth and steady state stages of thermohaline intrusions in the Arctic Ocean. *J. Geophys. Res.* **106**: 16,783–16,794.
- MCLAUGHLIN, F. A., E. C. CARMACK, R. W. MACDONALD, AND J. K. B. BISHOP. 1996. Physical and geochemical properties across the Atlantic/Pacific water mass front in the southern Canadian Basin. *J. Geophys. Res.* **101**: 1183–1197.
- MEI, Z.-P., AND OTHERS. 2002. Physical control of spring–summer phytoplankton dynamics in the North Water, April–July 1998. *Deep Sea Res. II* **49**: 4959–4982.
- MELLING, H., Y. GRATTON, AND R. G. INGRAM. 2001. Oceanic circulation within the North Water Polynya in Baffin Bay. *Atmos.–Ocean* **39**: 301–325.
- MENDEN-DEUER, S., AND E. J. LESSARD. 2000. Carbon to volume relationships for dinoflagellates, diatoms and other protist plankton. *Limnol. Oceanogr.* **45**: 569–579.
- MIDDELBOE, M., T. G. NIELSEN, AND P. K. BJØRNSSEN. 2002. Viral and bacterial production in the North Water: In situ measurements, batch culture experiments and characterization and distribution of a virus–host system. *Deep-Sea Res. II* **49**: 5063–5079.
- MONTAGNES, D. J. S. 1996. Growth responses of planktonic ciliates in the genera *Strobilidium* and *Strombidium*. *Mar. Ecol. Prog. Ser.* **130**: 241–254.
- , A. J. POULTON, AND T. M. SHAMMON. 1999. Mesoscale, finescale and microscale distribution of micro- and nanoplankton in the Irish Sea, with emphasis on ciliates and their prey. *Mar. Biol.* **134**: 167–179.
- NUSCH, E. A. 1980. Comparison of different methods for chlorophyll and phaeopigment determination. *Arch. Hydrobiol. Beih. Ergebn. Limnol.* **14**: 14–36.
- NOBLE, R. T., AND J. A. FUHRMAN. 1998. Use of SYBR Green I for rapid epifluorescence counts of marine viruses and bacteria. *Aquat. Microb. Ecol.* **14**: 113–118.
- PORTER, K. G., AND Y. S. FEIG. 1980. The use of DAPI for identifying and counting aquatic microflora. *Limnol. Oceanogr.* **25**: 943–948.
- RICHARDSON, K., M. F. LAVIN-PEREGRINA, E. G. MITCHELSON, AND J. H. SIMPSON. 1985. Seasonal distribution of chlorophyll *a* in relation to physical structure in the western Irish Sea. *Oceanol. Acta* **8**: 77–86.
- ROTH, B. L., M. POOT, S. T. YUE, AND P. J. MILLARD. 1997. Bacterial viability and antibiotic susceptibility testing with SYTOX green nucleic acid stain. *Appl. Environ. Microbiol.* **63**: 2421–2431.
- SATHYENDRANATH, S., A. LONGHURST, C. M. CAVERHILL, AND T. PLATT. 1995. Regionally and seasonally differentiated primary production in the North Atlantic. *Deep-Sea Res. I* **42**: 1773–1802.
- SCULLY, N. M., AND W. L. MILLER. 2000. Spatial and temporal dynamics of colored dissolved organic matter in the North Water Polynya. *Geophys. Res. Lett.* **27**: 1009–1011.
- SCHUSTER, S., AND G. J. HERNDL. 1995. Formation and significance of transparent exopolymeric particles in the northern Adriatic Sea. *Mar. Ecol. Prog. Ser.* **24**: 227–236.
- SHERR, B. F., P. DEL GIORGIO, AND E. B. SHERR. 1999. Estimating abundance and single-cell characteristics of respiring bacteria via the redox dye CTC. *Aquat. Microb. Ecol.* **18**: 117–131.
- SHIMETA, J. 1993. Diffusional encounter of submicrometer particles and small cells by suspension feeders. *Limnol. Oceanogr.* **38**: 456–465.
- SIMON, M., B. C. CHO, AND F. AZAM. 1992. Significance of bacterial biomass in lakes and the ocean: Comparison to phytoplankton biomass and biogeochemical implications. *Mar. Ecol. Prog. Ser.* **86**: 103–110.
- TALPSEPP, L., J. PAVELSON, T. PÖDER, K. KÜNNIS, K. PIIRSOO, AND V. PORGASAAR. 1999. On water masses and biological variability in the central and eastern Skagerrak during SKAGEX-90: Inflow of Atlantic water. *Fisk. Havet* **9**: 1–31.
- TARRAN, G. A., M. V. ZUBKOV, M. A. SLEIGH, P. H. BURKILL, AND M. YALLOP. 2001. Microbial community structure and standing stocks in the NE Atlantic in June and July of 1996. *Deep-Sea Res. II* **48**: 963–985.
- TSUJI, T., AND T. YANAGITA. 1981. Improved fluorescent microscopy for measuring the standing stock of phytoplankton including fragile components. *Mar. Biol.* **64**: 207–211.
- UNESCO. 1983. Algorithms for computation of fundamental properties of sea water. UNESCO Tech. Pap. Mar. Sci. **44**: 53.
- WHITE, D. 2000. *The physiology and biochemistry of prokaryotes*, 2nd ed. Oxford Univ. Press.
- WOMMACK, K. E., AND R. R. COLWELL. 2000. Viroplankton: Viruses in aquatic ecosystems. *Microbiol. Mol. Biol. Rev.* **64**: 69–114.
- WRIGHT, S. W., AND R. L. VAN DEN ENDEN. 2000. Phytoplankton community structure and stocks in the East Antarctic marginal ice zone (BROKE survey, January–March 1996) determined by CHEMTAX analysis of HPLC pigment signatures. *Deep-Sea Res. II* **47**: 2363–2400.
- ZWEIFEL, U. L., AND Å. HAGSTRÖM. 1995. Total counts of marine bacteria include a large fraction of non-nucleoid-containing bacteria (ghosts). *Appl. Environ. Microbiol.* **61**: 2180–2185.

Received: 11 January 2002

Accepted: 27 June 2002

Amended: 19 July 2002